Hydrological Sciences Journal

ISSN: (Print) (Online) Journal homepage: https://www.tandfonline.com/loi/thsj20

An approach to map karst groundwater potentiality in an urban area, Sete Lagoas, Brazil

Rafael Magnabosco, Paulo Galvão & Ana Maciel de Carvalho

To cite this article: Rafael Magnabosco, Paulo Galvão & Ana Maciel de Carvalho (2020) An approach to map karst groundwater potentiality in an urban area, Sete Lagoas, Brazil, Hydrological Sciences Journal, 65:14, 2482-2498, DOI: 10.1080/02626667.2020.1802031

To link to this article: https://doi.org/10.1080/02626667.2020.1802031

HYDROLOGICAL SCIENCES JOURNAL
2020, VOL. 65, NO. 14, 2482–2498
https://doi.org/10.1080/02626667.2020.1802031

An approach to map karst groundwater potentiality in an urban area, Sete Lagoas, Brazil

Rafael Magnabosco[a], Paulo Galvão[b] and Ana Maciel de Carvalho[c]

[a]Department of Geology, Federal University of Ouro Preto, Ouro Preto, Brazil; [b]Department of Geology, Federal University of Minas Gerais, Belo Horizonte, Brazil; [c]Science and Technology Institute, Federal University of Jequitinhonha and Mucuri Valleys, Diamantina, Brazil

ABSTRACT

Due to complex hydrogeological contexts, mapping groundwater potential zones in karst regions is a difficult task. This study was conducted on a karst terrain in Sete Lagoas, Brazil, where rapid urban growth without adequate water resources management resulted in the drilling of unproductive wells and possible aquifer over-exploitation due to the concentration of wells. The objective was to develop a method for mapping groundwater potentiality for karst aquifers, serving as water resources management tool, based on 3D geological modelling, field work and pumping test data, remote sensing, geophysics analysis and production of thematic maps, resulting in the hydrogeological conceptual model. The groundwater potentiality map showed that most potential zones are on the central area, limited by grabens, where limestones are in contact with unconsolidated sediments, on areas with higher density of morphostructural and geophysical lineaments, mainly in east–west and north–east directions, near karst surface features, on thicker karstified zones, with higher recharge rates.

ARTICLE HISTORY
Received 23 February 2020
Accepted 15 June 2020

EDITOR
A. Fiori

ASSOCIATE EDITOR
G. Jeelani

KEYWORDS
karst aquifer; groundwater potentiality; hydrogeological conceptual model; Sete Lagoas; geomodeller

1 Introduction

Karst aquifers are known for their capacity for storing large amounts of water, which means that hydrogeological studies are increasingly important, especially in terms of groundwater exploration and water supply. In Europe, karst lands cover 35% of the area, with cities such as London, Paris, Rome, Malaga and Vienna being partially or fully supplied by karst water resources, as well as in the United States, where 40% of the country's surface area is covered by this type of terrain (Ford and Williams 2007). In Brazil, it is estimated that 5% to 7% of the surface is covered by karst rocks (Karmann 1994). The municipality of Sete Lagoas (state of Minas Gerais) has the same hydrogeological context, where almost all the water public supply is caught from the local karst aquifer (Galvão *et al.* 2015).

Karst network development complexity, combined with the great spatial variability of the hydrodynamic parameters, leads to a highly heterogeneous and anisotropic aquifer system, thus making its investigation difficult (Goldscheider and Drew 2007). Nevertheless, it is possible to identify certain karstification patterns, which are developed at the intersection between rock's main fractures and its bedding planes, following regional hydraulic gradients, resulting in the main orientation and position of the conduits. Filipponi (2009) defined three types of horizons that control the karstification process, which are related to 1) the mineral composition of the strata (e.g. presence of pyrite) contributing to water acidification, favouring dissolution and karstification; 2) contacts of strata, lithologies or facies with contrasted permeabilities; and 3) fractures that developed parallel to the bedding plane, increasing local permeability, which is the main feature controlling the karstification process in Sete Lagoas (Galvão *et al.* 2017).

The hydrogeological context of Sete Lagoas municipal area consists of the Archaean-fractured crystalline aquifer (Belo Horizonte Complex Basement), covered by the Sete Lagoas karst aquifer (the main water resource that supplies the city) and the Serra de Santa Helena aquitard, both of Neoproterozoic age, and the porous media aquifer composed of Cenozoic unconsolidated sediments (Pessoa 1996, Galvão 2015). Due to the connection between those aquifers in some areas, they can be classified into a karst-fractured aquifer system, where almost all groundwater flows in karst conduits developed mainly in limestone enlarged bedding planes and subvertical fractures.

Due to the great groundwater availability, the proximity to the state capital and availability of limestone for quarrying, the municipality of Sete Lagoas has attracted important economic activities (industries, mining and agriculture), resulting in an accelerated urban growth without effective water resources planning (Alves *et al.* 2007, Landau *et al.* 2011). Consequently, there is a high concentration of wells especially in the central urban area, resulting in a large cone of depression caused by high pumping rates, which also contributes to increased geotechnical risks (Galvão *et al.* 2015). Besides, there are constant reports of lack of water and dry wells, especially during drought periods, between April and September, as well as issues related to drilling new wells with low pumping rates, causing financial losses to the city.

Therefore, the development of a method for mapping groundwater potential zones is important and could help to

CONTACT Rafael Magnabosco de Almeida Gomes rmalmeidagomes@gmail.com Department of Geology, Federal University of Ouro Preto, Ouro Preto, MG 35400-000, Brazil

improve water resources management. There are several studies applying theoretical or empirical methods to groundwater potential mapping developed for porous aquifers (Niedzielski Andrea 2013), fractured aquifers (Madrucci *et al.* 2008, Ayer *et al.* 2017, Brito 2018), and karst aquifers (Saied. 2008) according to their local features. A detailed study should be developed for the municipality of Sete Lagoas considering its hydrogeological and hydraulic features in a context of tropical karst aquifer system.

The goal of this paper is to develop a method to map and assess groundwater potential zones in an urban karst aquifer, that can be used in other regions, highlighting areas with a greater likelihood of finding groundwater, based on a detailed hydrogeological conceptual model that supports a GIS-based index model through a weighted ranking system. The final map can be used as a tool for planning urban expansion, solving environmental and geotechnical issues related to well concentration and water overexploitation.

2 Site description

The study area is about 252 km^2 and it is in the central portion of the municipality of Sete Lagoas, 70 km northwest from the capital of the state of Minas Gerais, Belo Horizonte, Brazil (Fig. 1). Sete Lagoas has approximately 236,000 inhabitants (IBGE–Brazilian Institute of Geography and Statistics 2016), making it a medium-sized city which has developed very fast, presenting an accelerated urban growth, due to the industrial, agricultural and service sectors, besides limestone mining and metallurgical companies (Alves *et al.* 2007, Landau *et al.* 2011). Public water supply is managed by the Water and Sewerage Service [SAAE – *Serviço Autônomo de Água e Esgoto*] using almost exclusively groundwater from public wells (Galvão *et al.* 2015). So far, 115 public wells have been drilled within the study area, in addition to 198 private ones, resulting in 313 wells. A great number of these wells (32%) are in the central urban area, causing significant water level decrease in the region (Galvão *et al.* 2015).

Geologically, the area is in the extreme southeast of the São Francisco Craton, consolidated at the end of the Brasiliano Neoproterozoic orogeny, delimited by the Araçuaí and Brasília belts (Almeida 1977, Alkmim *et al.* 1993). The basement occurs in the southern region of the municipality, composed of gneissic or granitoid rocks and migmatized zones (CPRM 2003, Tuller *et al.* 2010). The Bambuí Group overlays the basement, represented from base to top by the Neoproterozoic formations Sete Lagoas and Serra de Santa Helena. The Sete Lagoas Formation is subdivided into two members: 1) Pedro Leopoldo, at the base, composed of calcilutite and calcisiltite with sub-horizontal bedding planes intercalated with mudstones and dolomites strata; and 2) Lagoa Santa, on top, composed of fine- to medium-grained calcarenites (Pessoa 1996). The Serra de Santa Helena Formation covers most of the area, consisting mainly of fine laminated clayey siltstones, with millimetre intercalations of mudstone and fine sandstone. Overlapping the Bambuí Group are the Cenozoic unconsolidated sediments, occurring mainly in the central region of the municipality and over river drainages and terraces (Tuller *et al.* 2010, Galvão *et al.* 2016) (Fig. 1).

There were at least three geotectonic and structural deformation stages: 1) extensional, characterized by NNW–SSE high-angle extensional faults, dipping to east, which progressed

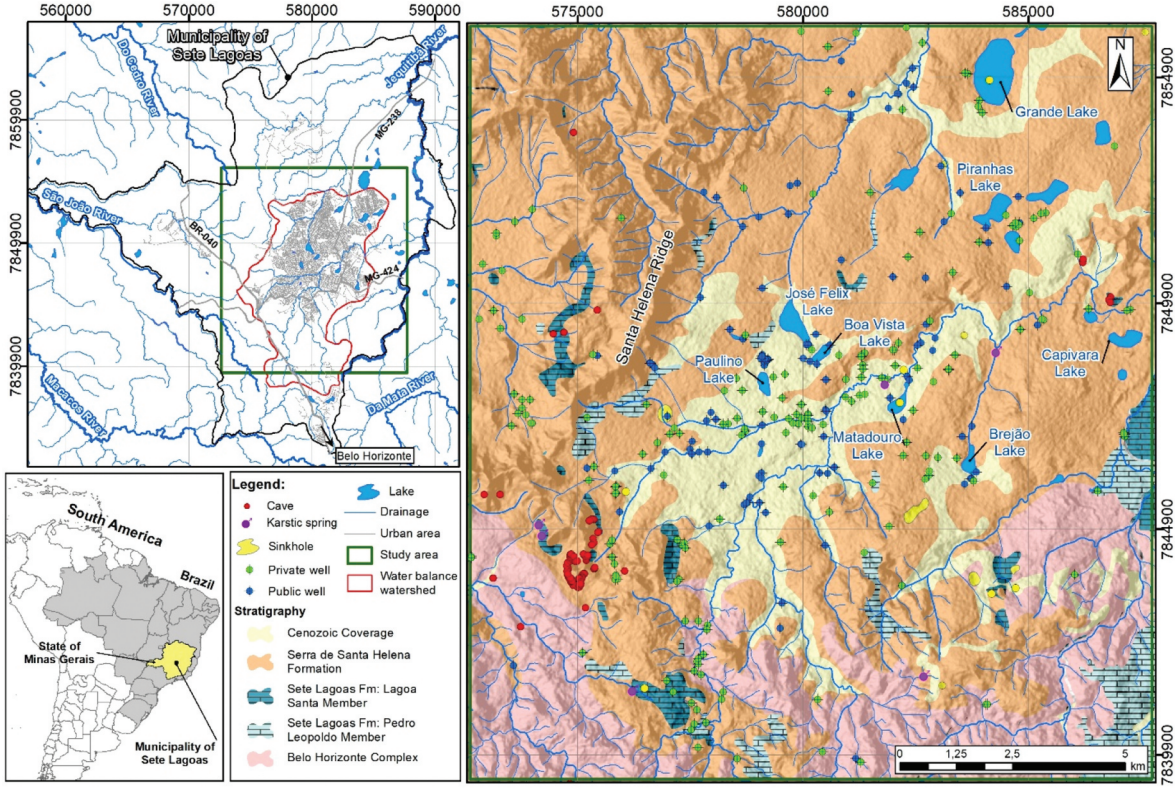

Figure 1. Locations of the municipality of Sete Lagoas (bottom, left), the study area (green area, top, left) and the respective geological information and karst features.

during the initial sedimentation of the Bambuí Group's carbonic-pelitic sequence; 2) compressive, evidenced by the low angle compressive shear to west, parallel to the stratification planes, causing bedding planes transposition. The main orientation is around N–S and there was no basement involvement, characterizing thin-skinned tectonics; and 3) distensive, related to extensional basement block movements that generated deformation of supracrustal rocks, resulting in antiform and synform folds with E-W axis and rotation of previously formed structures (CPRM 2003).

The climate is tropical semi-humid, usually hot with rainy summers and dry winters. The average annual rainfall is 1321 mm, with a cumulative rainfall of 1183 mm from October to March, representing 90% of annual precipitation. The average annual temperature is 21.7ºC, whereas July has the lowest monthly average value (18.3°C), and February the highest one (23.7°C) (INMET–National Institute of Meteorology 2019). The climatological water balance shows a water surplus around 406 mm/year (~31% of the precipitation), occurring between December and March. The largest water deficits occur in August and September. Soil water replenishment begins in November, when precipitation becomes greater than evapotranspiration, until it reaches the soil water capacity (Pessoa 1996).

The geomorphological pattern is related to local karst geology, presenting caves, sinkholes, lakes, few surface drainages and closed drainage basins, as well as a hilly relief pattern and dendritic drainage developed on low permeability pelitic rocks and on basement areas. The elevation of the area ranges from 1070 to 670 m, decreasing to the northeast. As occurs in karst terrains, the local lakes usually occupy depressions in the overlying unconsolidated sediments, which are caused by slumpage into sinkholes at depth, keeping connections with the underneath karst aquifer, exemplified by the Matadouro and Grande lakes (Assunção 2019). Galvão *et al.* (2017) also showed that some lakes may contribute to karst aquifer recharges due to the presence of nitrate and stable isotope evaporation signatures on groundwater samples that are similar to the water from the lakes, such as in the José Felix, Brejão, Grande and Piranhas lakes (Fig. 1). However, some lakes were anthropized as the city hall modified their substrates, covering with fine material to seal the infiltration of water, like in the Boa Vista and Paulino lakes.

The municipality is in the Paraopeba and Velhas river basins, separated by the Santa Helena ridge, both belonging to the São Francisco River basin. The most important subbasin for Sete Lagoas is the Jequitibá watershed, which drains the entire urban area and most of the study area, bordering the eastern limit of the municipality and flows towards the Velhas River (Fig. 1).

Pessoa (1996) and Galvão (2015) classified the region into four hydrostratigraphic units, from bottom to top: basement fractured aquifer, Sete Lagoas karst aquifer, Serra de Santa Helena aquitard, and the Upper Cenozoic porous aquifer. Since the karst aquifer is connected to the basement fractured aquifer, especially close to normal faults, it can be considered as a karst-fractured aquifer system, with very different properties and flow conditions. In the central region, the porous aquifer may also be in connection with the karst aquifer due to a depositional gap or erosion of rocks of the Serra de Santa Helena Formation (Galvão *et al.* 2016). Therefore, the karst aquifer is unconfined in areas with Cenozoic unconsolidated sediments and confined when it is overlapped by the rocks of the Serra de Santa Helena Formation. The recharge of karst aquifer is derived from a mixed autogenic-allogenic basin, with slow infiltration through the weathering mantle or fractures from the basement and metapelitic rocks, and autogenic through sinkholes, caves, limestone outcrops and the Cenozoic unconsolidated sediments. The main discharge of karst aquifer within the basin (red watershed in Fig. 1) is by well abstraction, since there are few karst springs with low discharges, representing a small percentage of the total.

The limestone matrix has almost no total porosity nor hydraulic conductivity, around 3% (Peñaranda 2016) and 10^{-9} m/s (Galvão *et al.* 2015), respectively. Consequently, groundwater flow in the karst aquifer is almost entirely limited to open conduits and fractures (Galvão *et al.* 2015). The conduits developed preferentially between enlarged bedding planes and subvertical limestone fractures (Galvão 2015, Ribeiro *et al.* 2016), being the main karstification zones. Regarding the fractured basement aquifer and the Serra de Santa Helena aquitard, the water percolates through weathering mantle and subvertical fractures, whose flow conditions, storage, and permeability depend mainly on the density and interconnectivity of the fractures, on their aperture and whether they are filled or not. The porous aquifer, composed of Cenozoic unconsolidated sediments, has slower flow velocity but a good storage capacity (Pessoa 1996).

3 Materials and methods

The study is divided into four steps: (1) data processing; (2) remote sensing and geophysical analysis; (3) geological modelling, and (4) thematic maps production. In the first stage, data of topography, hydrography and geomorphology, in addition to well profile features, water level, hydrodynamic parameters, as well as surface geology (geological map) and subsurface data (lithological profiles and camera inspections) were collected, which made it possible to model the hydrostratigraphic units' geometry. Remote sensing and geophysical analysis, based on the delimitation of morphostructural and geophysical lineaments, were essential for the interpretation of main geological structures in the model, as well as serving as a database in thematic maps. The combination of existing information with those developed in geological modelling, remote sensing and geophysical analysis allowed the production of four thematic maps: (a) density of lineaments and well productivity, (b) recharge map, (c) potentiometric surface and wells influence, and (d) karst groundwater potentiality map. The thematic maps and geological model constitute the hydrogeological conceptual model described in the results and discussion of this paper. The steps are detailed below.

3.1 Data processing

The topography was taken from Alos Palsar elevation raster of the Japanese Aerospace Service (JAXA), with a spatial resolution of 12.5 m, corrected with the ArcToolbox Fill tool. An

analytic signal amplitude geophysical image was used in the lineaments delimitation and derives from the airborne magnetometry database belonging to CODEMIG (Company of Economic Development of Minas Gerais), area 10 (Belo Horizonte-Curvelo-Três Marias). A 10 m resolution image from Sentinel 2 satellite was obtained from the Alaska Satellite Facility (Copernicus Sentinel Data 2018) to produce an NDVI (Normalized Difference Vegetation Index) map. The geological map was a compilation between the maps of Galvão (2015), scale 1:25,000, and CPRM (2003), scale 1:50,000. Cave entrances and sinkholes locations were acquired from the National Center Research and Cave Preservation (CECAV 2009), plus the sinkholes mapped by Assunção (2019). The drainage and lakes were taken from the National Water Agency (ANA 2017), and karst springs from Pessoa (1996). Precipitation and temperature data were taken from the climatological and weather station of Sete Lagoas (INMET–National Institute of Meteorology 2019).

Tubular wells data was provided by the Water and Sewerage Service of Sete Lagoas (SAAE–http://www.saaesetelagoas.com.br/), Integrated Environmental Information System of Minas Gerais (SIAM–http://www.siam.mg.gov.br/siam/login.jsp) and Groundwater Information System from Brazil (SIAGAS–http://siagasweb.cprm.gov.br/layout/), resulting in 313 wells. Among these wells, 161 contain lithological information and Galvão (2015) realized camera inspections on 30 of them, plus 24 step-drawdown tests and nine long-term aquifer tests. Static water levels (SWL) were obtained in 68 wells from Pessoa (1996), while stabilized dynamic water levels (DWL) were measured in 54 wells during field work in September 2017.

Specific capacity (Q/s) were compiled from 161 well drilling reports and 24 step-drawdown tests, resulting in 185 Q/s values. Transmissivity (T) values were taken from 22 monitoring wells by long-term aquifer tests and 10 were estimated by Galvão *et al.* (2015) using empirical relationship analysis with Q/s, resulting in a total of 32 T values. These two parameters were considered as an estimation of well productivity, as they can indicate the amount of groundwater a well is capable of withdrawal in a period and in a given water level lowering. Although specific capacity is not reliable as transmissivity, because it depends not only on the aquifer properties, but also on conditions of the well, reflecting in its efficiency, being an indirect approach of groundwater potential that can provide reliable trends. Besides, as the wells completion within the area are similar, the well's efficiencies are also comparable. Despite most of wells, reports did not have enough data to calculate the well's efficiency, Galvão (2015) did it for the 24 step-drawdown tests, resulting in a median of well efficiency of 71%. These wells were correlated with the hydrogeological and structural context of the area in thematic maps, making possible to compare well productivity with groundwater potentiality.

3.2 Remote sensing and geophysical analysis

Remote sensing and geophysical analyses were performed to map regional lineaments, since they are considered important features for understanding the geotectonic and hydrogeological contexts of the region (O'Leary *et al.* 1976, Cook 2003). Lineaments can be strongly related to deeper structures, such as faults, fractures, and basement slope (Pessoa 2005), acting as a potential flow path for groundwater circulation and/or storage, and hence for high well productivity (Alonso-Contes 2011, Mendes *et al.* 2016).

For morphostructural lineament mapping, digital terrain models (generated by ArcToolbox Hillshade tool) were used with a spatial resolution of 12.5 m, sun illumination angle of 0 and 270 degrees, and 2x vertical exaggeration, in addition to satellite images taken from Google Earth. Surface structures, such as sharp topographic unevenness, linear drainages, ridges, lakes alignments were mapped as morphostructural lineaments, highlighting shallow rock structures like bedding plane, fractures, foliation or the intersection between them.

The geophysical analysis was carried out on a magnetometric analytical signal amplitude map (ASA), whose anomalies are clearer and more accurate, highlighting deep rock structures such as intrusive igneous bodies, faults, folds, geological contacts, grabens and horsts (Luiz and Silva 1995). The geophysical lineaments were mapped at the centre or on the edge of ASA anomalies.

These structures were grouped to make the lineament density map using ArcGIS Kernel Density tool. Statistically, kernel density estimation is a non-parametric way to estimate the probability density function of a random variable. It was considered that each lineament would have a population value of 1, with a search radius of 1000 m and planar method, due to the better adaptation with the size of the area and working scale. The density in each cell was calculated by adding values of all overlapping surfaces, resulting in the unit of km/km^2 of lineaments. Subsequently, morphostructural and geophysical lineaments were analysed in a rosette diagram using Rockworks 17 software to verify their main directions.

3.3 Geological modelling

The geological modelling was performed with Geomodeller software, which uses lithological contacts and structural data in a potential field method to perform geostatistical interpolation (cokriging) of implicit surfaces, resulting in a 3D model (Cowan *et al.* 2003, Calcagno *et al.* 2008, Hassen *et al.* 2016). Geological map with surface karst features, 161 lithological well profiles, 30 camera inspections, field-measured structural data by CPRM (2003) and Galvão *et al.* (2016), and morphostructural and geophysical lineaments were the information considered for the modelling.

The model domain has dimensions of 15,113 m x 16,669 m (green polygon in Fig. 1), ranging from 450 m to 1200 m of elevation. Six hydrogeological units were represented: 1) Basement, corresponding to the Belo Horizonte Complex; 2) Sete Lagoas Formation, composed of compact limestones; 3) Karstified zones, representing the connection between sinkholes, caves, fractures, and conduits; 4) Serra de Santa Helena Formation, consisting of mudstones; 5) Epikarst, representing weathered limestone; and 6) Unconsolidated sediments, which refer to medium-coarse-grained sandy-conglomeratic material and silt. The karstified zones were identified as the intervals of water inflows, fractures, cracks or cavities described in lithological well profiles and camera inspections and connected

with surface karst features. Morphostructural and geophysical lineaments were used coupled with tectonic and structural regional study and lithological well profiles to infer normal faults and the geometry of the basement.

Geological modelling provided information about the geometry of the hydrostratigraphic units, showing the position of the main karstified zones, fractures and faults trends, thicknesses and elevations of the layers, which were exported and used in the production of the groundwater potentiality map. Statistical treatment of the data with ArcGIS helped to estimate the maximum, minimum and average of thickness and elevation of all layers in the conceptual hydrogeological model.

3.4 Thematic maps

3.4.1 Aquifer recharge and water balance

The recharge map production was based on the APLIS method (Andreo *et al.* 2008), which was tested in karst aquifers with different characteristics, compared with other methods established in the literature and validated with the average annual discharge rate of each aquifer. The method advantage is a spatial distribution of the recharge rate (precipitation in %) consistent with the karst aquifer features, such as autogenic recharge in sinkholes or caves, fracture or karstification intensity.

As the recharge map is considered a parameter to estimate the water balance of the city of Sete Lagoas strictly, i.e., compare the amount of inflow and outflow water of the karst aquifer in the urban area, premises that helped to delimit the basin used in the calculations were established. Firstly, the basin chosen to produce the recharge map considered the entire catchment area and the hydrogeological boundary conditions upstream the city to guarantee that all the inflow water in the urban area would be computed in the water balance. Due to the connection between the karst aquifer and the basement fractured aquifer (Galvão *et al.* 2017), sectors where the basement rocks outcrop in the South were also considered as a recharge area for mapping. Secondly, as the main karst aquifer discharge in the area is the withdrawal of groundwater by wells, it was acceptable to use the city's contour, respecting hydrogeological conditions, such as potentiometry, topography and lithology, to delimit and close the basin downstream (red watershed in Fig. 1). Therefore, all the inflow and outflow water of the karst aquifer in the urban area were considered, fulfilling the objective of estimating the water balance of the city and not the entire hydrographic basin, as did Pessoa (1996).

The method considers six parameters, resulting in six maps (Fig. 2): altitude (A), slope (P), lithology (L), infiltration landforms (I), soil type (S), and hydrogeological unit correction factor (Fh). These parameters were classified according to the weights of Table 1, following the APLIS method with some adaptations explained below.

In the infiltration landforms map, weight 10 was assigned to the region of caves and sinkholes due to autogenic recharge; weight 5 to the morphostructural lineaments and lakes with leakage, because of their connection with karst aquifer by subsurface structures; and weight 1 to the anthropized lakes or those not connected with karst aquifer, i.e., with low permeability material on their base, and the remaining areas.

The soil type map was replaced by a normalized difference vegetation index (NDVI) classification map, as there was no detailed pedological map in the region, and to consider other important features such as exposed limestone mining regions, vegetation type and urban area. In order to elaborate this NDVI map, red and infrared bands of 10 m spatial resolution

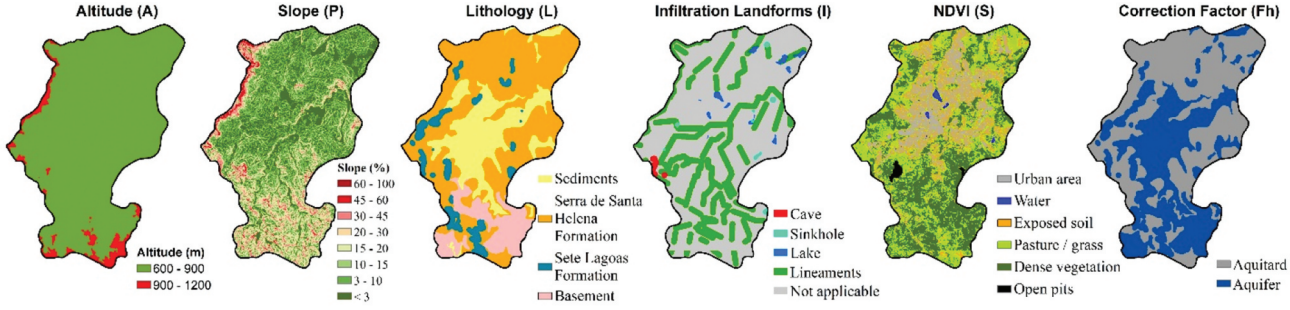

Figure 2. Criteria used in the APLIS method for recharge map.

Table 1. Parameters weights used in APLIS method for recharge map.

Altitude (m)		Slope (%)		Lithology		Infiltration landforms		NDVI	
<300	1	<3	10	Limestone	8	Sinkholes	10	Mining and exposed rocks	10
300–600	2	3–5	9	Mudstones	1	Caves	10	Dense vegetation	8
600–900	3	5–10	8	Unconsolidated sediments	4	Morphostructural lineaments	5	Undergrowth or pasture	5
900–1200	4	10–15	7	Basement	2	Lakes connected with karst aquifer	5	Exposed soil	4
1200–1500	5	15–20	6			Non-connected lakes	1	Surface water	2
1500–1800	6	20–30	5			Remaining area	1	Urban area	1
1800–2100	7	30–45	4						
2100–2400	8	45–60	3						
2400–2700	9	60–100	2						
>2700	10	>100	1						

from Sentinel-2 satellite image were used, as explained by Moura *et al.* (2017).

The correction factor map subdivides the region into aquifers and non-aquifers. The regions considered as aquifers are those where there are limestone, basement or areas covered by unconsolidated sediments, therefore weight 1. The Serra de Santa Helena Formation was considered as an aquitard, with weight 0.1. The classification of the remaining maps (altitude, slope and lithology) is in accordance with the APLIS method (Andreo *et al.* 2008). Finally, the recharge was computed using the Equation 1:

Recharge

$$(\%\ \text{of precipitation}) = [(A+P+3L+2I+S)/0.9] \times Fh \qquad (1)$$

The computed water balance of the karst aquifer within the study area was based on water inflow minus water outflow, i.e., annual recharge volume minus annual well water exploitation and karst springs discharges. For this, the area and recharge rate of each pixel of the recharge map was multiplied by the annual average precipitation to obtain the total annual recharge volume. The discharge was calculated by multiplying the flow rate of 204 active wells within the basin by the pumping rate per year, resulting in the annual volume of exploited water. To verify if those wells are truly active, it was considered only public and private wells classified as "equipped", "active wells", "legal granted wells" or "ongoing grant processes", based on data from SIAGAS, SAAE and SIAM. Discharge rates of public wells were measured in May 2018 by using an ultrasonic flowmeter and, for those not measured in fieldwork, well water license processes were consulted. The pumping rate was also provided by the same public entities and for those without the data of pumping rate the average was used. The discharges of karst springs were measured only once in the dry season of 1991 by Pessoa (1996). As they can increase in rainy season, they were considered as the minimum annual discharges, representing a small percentage of the total discharge of the study area.

The mean annual evapotranspiration and water surplus were calculated in the climatological water balance using the method of Thornthwaite and Mather (1955), which were used to find the surface runoff by subtracting the recharge from the water surplus.

3.4.2 Potentiometric surface and well influence

The potentiometric surface map was based in 68 wells, by using Pessoa (1996) measurements of the static water level (SWL) in 1991. The hydraulic head was recalculated by subtracting the depth of SWL from the elevation of each well extracted from the topographic surface data used in this study. Another potentiometric surface map was made, influenced by water withdrawals, considering the stabilized dynamic level from 54 wells measured in September 2017. For both maps, only wells intercepting the Sete Lagoas karst aquifer were selected for hydraulic head calculations. The surfaces were interpreted and adjusted according to topography and geological model boundary conditions, such as faults or contact with the basement.

3.4.3 Method to map groundwater potentiality in karst aquifer

The groundwater potentiality map was based on a parametric analysis performed by means of weighting, classifying and interpolating parameters represented in maps. Similar methods were used by Madrucci *et al.* (2008), Pirasteh and Saied. (2008), Niedzielski Andrea (2013), Ayer *et al.* (2017), and Brito (2018).

Firstly, it was necessary to define which parameters represent best the hydrogeological features that control the groundwater potentiality (GP) of the karst aquifer, that might represent the same features in other karst aquifers. Thus, some assumptions were established to select these parameters considering the karst aquifer features observed in the geological model, thematic maps and the structural-geological and hydrogeological contexts of karst aquifers recorded in the scientific literature: (1) open fractures and conduits are the structures with most porosity and permeability in this type of aquifer, which are necessary in groundwater exploration, and they govern the groundwater flow direction (Ford and Williams 2007). As Filipponi (2009) explained, the karstification process can be controlled by the mineral composition of the strata, contrasted permeabilities of contacts, lithologies or facies, and fractured bedding plane; (2) morphostructural and geophysical lineaments are intrinsically related to the regional structural-geological context by representing shallow and deep structures present in rocks (O'Leary *et al.* 1976, Cook 2003, Melo *et al.* 2015, Salles *et al.* 2018), so the higher the lineaments density, the greater is the connectivity of structures, and hence the greater are the porosity, permeability and karstification; and (3) surface karst features, such as sinkholes, caves, dry valleys, streamsinks, resurgence, lapies are important indicators to karstified zones, as they are dissolution features that normally appear and develop in structures of the rock and connect the surface with the conduits network (Ford and Williams 2007).

Therefore, four parameters were established to map groundwater potentiality in karst aquifers (Fig. 3): (a) lineaments density; in this case, it was considered morphostructural and geophysical lineaments; (b) surface karst features density; (c) thickness and position of karstified zones; whatever the type of karstification, if it follows some contact, strata or other structures, the idea for this parameter is to map the underground karstified zones using lithological well profile, well logs or geophysics analysis, and represent them in estimated surfaces; and (d) recharge rates from APLIS method, because it comes indirectly with other features, such as lithology, infiltration landforms, slope, altitude, and type of soil, that is also important to map karst groundwater potentiality, since recharge rate and dissolution features are intrinsically related to underground karstified zones (more recharge, more water contributing to karstification).

Maps 1 and 2 were produced using the ArcToolbox Kernel Density estimation method, described in Section 3.2. However, in Map 1, the lineament density was calculated in km/km^2, while in Map 2 it was necessary to transform the surface karst features (sinkholes, caves, and some lakes) into points, resulting in points/km2. For Map 3, the thicknesses of the karstified zones 1 and 2 were exported from the geological model and summed to create

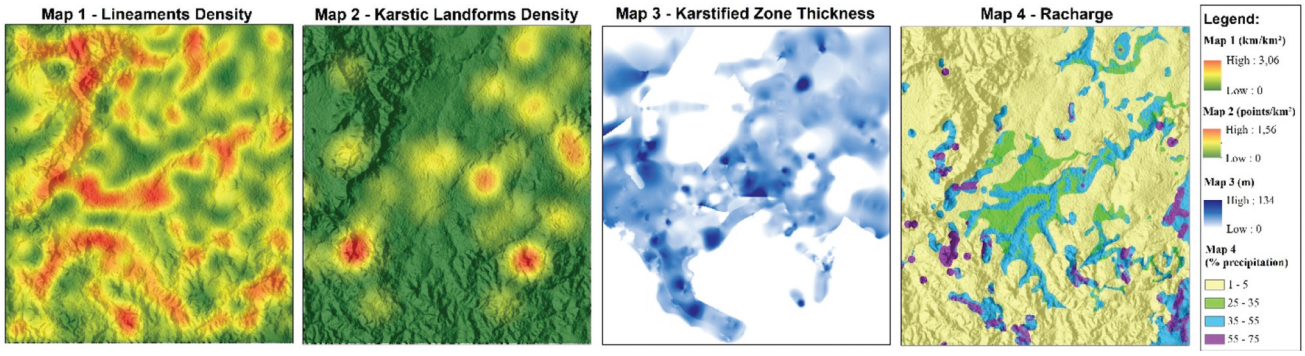

Figure 3. Main parameters assessed for karst groundwater potentiality map.

the map accumulated thickness of karstified zone. For the recharge map, the APLIS method described in Section 3.4.1 was used, with one exception that the areas where basement rocks outcrop were not considered in the calculations, as they are not part of the karst aquifer. Each of these 4 parameters were classified as "very low", "low", "moderate", "high", and "very high" groundwater potentiality classes (Table 2), trying to choose the best intervals for each parameter, evaluating the intervals numerically and also their spatial distribution on the map. It is important to note that this classification can change and depends on many factors, such as the amount of data, range of each parameter and their spatial distribution.

The maps were interpolated and a multiplication factor was assigned to each one according to its influence on the groundwater potentiality (GP) calculation, based on the back analysis of the specific capacity and transmissivity of the well that, theoretically, indicate the most productive regions of the aquifer. It is also possible to use a PEST (parameter estimation) software to determine the influence and weight of each parameter and their sensibility (Doherty 2004, Hunt *et al.* 2009). So, the multiplication factors were calibrated with 185 Q/s and 32 T values, adjusting the map until the interpolation yielded a suitable result. In other words, the location of the wells with higher specific capacities and transmissivities must correspond to the regions of greatest groundwater potentiality, while less productive wells should be in the lower potential areas. The maps were interpolated using Equation (2) in raster calculator tool from ArcGIS.

$$GP = \begin{pmatrix} 0.2 \times \text{Lineaments} \\ \text{density} \end{pmatrix} + \begin{pmatrix} 0.35 \times \text{Kars features} \\ \text{density} \end{pmatrix} + \begin{pmatrix} 0.25 \times \text{Karst zone} \\ \text{thickness} \end{pmatrix} + (0.2 \times \text{Recharge}) \quad (2)$$

The GP map was then classified into five classes, from "very low" to "very high", using the Equals Intervals symbology from ArcGIS. The correspondence of the GP map with well productivity was evaluated with a scatterplot, showing a linear relationship of specific capacity and transmissivity values with the groundwater potentiality classification.

4 Results and discussion

The following results deal with the interpretations regarding the geological model and thematic maps produced, consisting of a complement of the hydrogeological conceptual model elaborated by Pessoa (1996) and Galvão (2015).

4.1 Lineaments and structural geology

Figure 4 shows that the lineaments have two major directions: north–south, correlated with the main low angle foliations and westward compressive shear zones in limestones and mudstones; and east–west, associated with open fractures parallel to the main compressive stress σ1, corresponding to limestone mineral stretching lineation, and direction of the most frequent conduits registered by Ribeiro *et al.* (2016). Two secondary directions are also noted: N40–60 W, having similarity with the direction of the extensional faults in the basement and with the axis of graben and horst structures (Pessoa 2005), therefore more expressive in the geophysical lineaments; N20–60E, corresponding to fractures in the Bambuí Group, with some representative conduits mapped by Ribeiro *et al.* (2016) and groundwater flow directions noted by Auler (1994) using dye tracers. Other directions around NW and NE may be structure deviations caused by rocks with different competencies, such as basement ramps and horsts, or have been rotated by block sloping during distensive stages (CPRM 2003). It reveals the basement importance in shaping the lithostructural framework, corresponding to morphostructural compartments and regional lineaments (Pessoa 2005).

Table 2. Classification of the parameters used in the elaboration of the groundwater potentiality (GP) map.

Lineaments density (km/km²)	Karst features density (points/km²)	Karst zone thickness (m)	Recharge (%)	Weight	Classification
0–0.5	0–0.2	0	1–10	0	Very low
0.5–1	0.2–0.4	0–15	10–25	1	Low
1–1.75	0.4–0.8	15–30	25–40	2	Moderate
1.75–2.5	0.8–1.2	30–60	40–55	3	High
2.5–3	1.2–1.6	> 60	55–75	4	Very high
0.2	0.35	0.25	0.2	Multiplication factor	

There are at least two morphostructural lineament patterns: (a) the central and northeastern region, where the Bambuí Group rocks are thicker or covered by Cenozoic unconsolidated sediments, with poor drainage networks, and hence fewer lineaments (but larger) with east–west and NE directions; (b) In the Santa Helena ridge and in the southern region, although there are more lineament occurrences, they are smaller and in several directions, despite the ridge being structured in NW and NE directions.

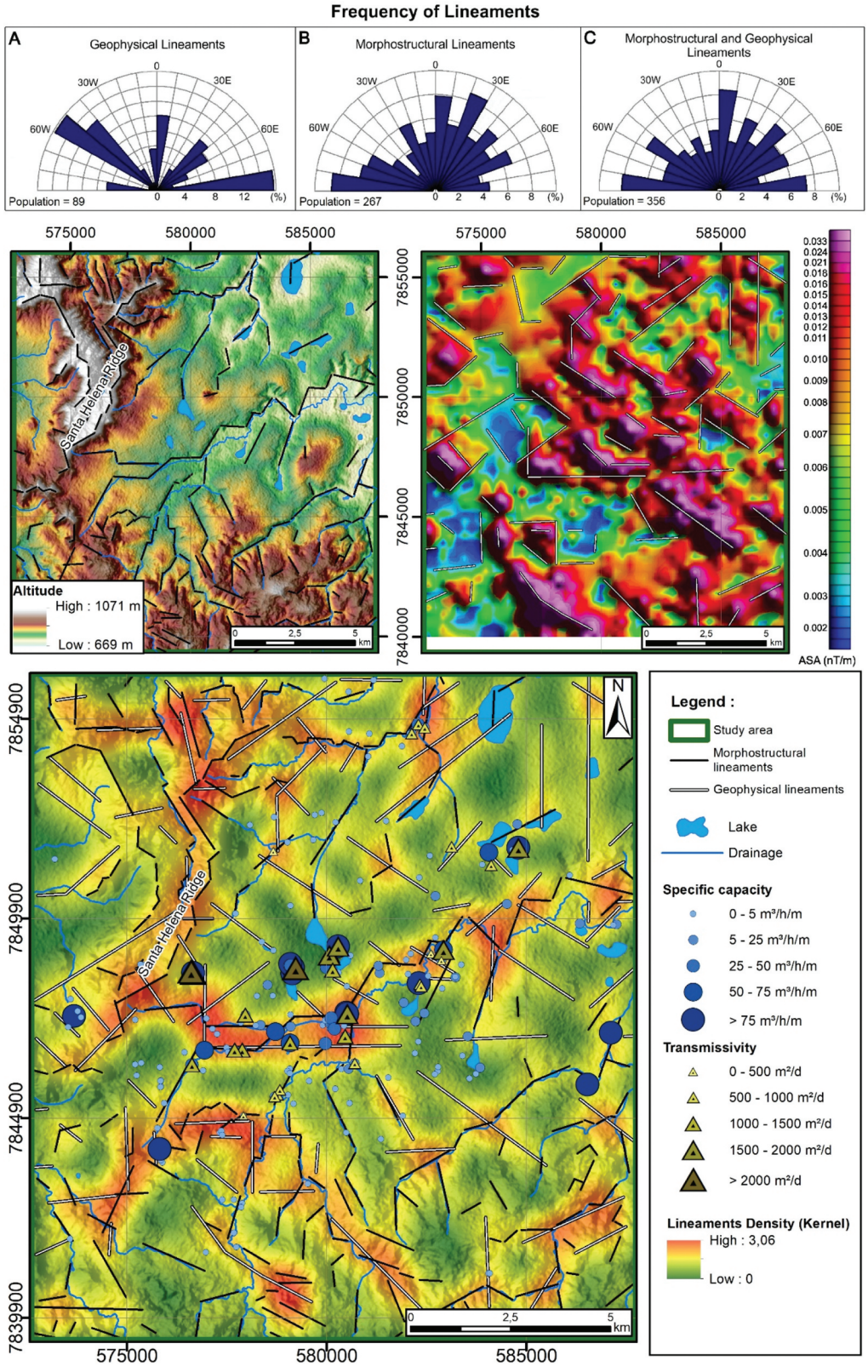

Figure 4. Remote sensing analysis and wells hydrodynamic parameters. Rosette diagrams and maps with the morphostructural and geophysical lineaments directions (top). Lineaments density map with specific capacity values and well transmissivity (bottom).

Regarding the geophysical lineaments, they have generally E-W and NW directions in the central region.

The lineament density map (Fig. 4) reveals that regions with higher lineament density are well correlated with the main directions seen in rosette diagrams, showing that the local geology corresponds to the regional geological context. The lakes in the area tend to follow the direction of the nearby morphostructural lineaments, which is expected, as most of the lakes are enlarged sinkholes that were filled with sediments and the alignment of karst features probably indicates groundwater flow direction due to karstification through limestone structures.

4.2 Aquifer geometry

The geological model (Fig. 5) occupies an area of 252 km^2, uniting the four main hydrostratigraphic units, from bottom to top: basement fractured aquifer; Sete Lagoas karst aquifer, represented by the compact and weathered limestone and karstified zones; Serra de Santa Helena aquitard, and unconsolidated porous aquifer. Two main karstified zones (KZ1, KZ2) were modelled to represent the connection between conduits, fractures, sinkholes and cave entrances (Table 3).

All hydrostratigraphic units follow the basement's dip, decreasing from south/southwest to north/northeast. The units' contacts are abrupt due to normal faults in graben/horst structures and due to the transposition of layers that formed shear zones at the compressive tectonic event. The basement relief in grabens and horsts, with main directions N60 W, N40E and E-W, played an important role in the later deformation process of limestones, acting as natural obstacles to the direction of transport, shaping lithostructural frameworks, corresponding to the morphostructural compartments and photo-interpreted lineaments (CPRM 2003, Pessoa 2005, Tuller *et al.* 2010).

The Sete Lagoas karst aquifer is outcropping mainly at the base of the Santa Helena ridge and in the southern region over basement horsts. The dimension and thickness of this aquifer can vary considerably due to the basement topography and fault reactivation. The karstified zones (KZ1 and KZ2 – Fig. 5) are developed mainly through the Sete Lagoas Formation bedding planes or in the basal detachment faults. However, the main conduits occur more specifically along the intersections between bedding planes and open subvertical fractures orientated E-W and N20-60E, corresponding to morphostructural and geophysical main lineament directions and groundwater flow directions found by Auler (1994).

The Serra de Santa Helena aquitard has an average thickness of 51 m but can reach up to 200 m in the ridge or in the north of the area. Its spatial distribution occurs almost in the entire area covering limestone, being absent in some regions, especially in the central area (Fig. 5).

The porous media aquifer was formed by the deposition of sandy sediments from alluvium and terraces or sandy clay layers with gravel interbeds (Pessoa 1996, Tuller *et al.* 2010). The grabens reliefs favoured the deposition of sediments in the central region, with an average thickness of 24 m, reaching up to 100 m especially near the fault zones. The connection with karst aquifer and the slow percolation of water through sediments, favouring the formation of humic acids, intensified the karstification in areas where limestone is covered only by sediments (Galvão *et al.* 2017).

The analysis of lithological well profiles reveals karstification near the basement contact, especially over horsts (Fig. 6, cross-sections 1–4), probably due to the basal detachment fault, reinforcing the premise of hydraulic connections between fractured and karst aquifers.

4.3 Potentiometric surface and well influence

The regional groundwater flow direction is to NE, with some local variations, especially in the northeastern portion of the area, where there is a slight eastward flow deviation. Hydraulic heads range from 820 m near cave entrances at the Santa Helena ridge foothills, in southwest, with hydraulic gradient of 2.5–6.0%, to 690 m in northeast of the map, near the Grande lake, with hydraulic gradient of 0.3–2.5% (Fig. 7). This difference probably exists due to the horsts and grabens structures, while the steeper hydraulic gradient is close to the ridge, where limestones were transported over the horsts, and the flatter is on depressions areas, where the limestones probably are more karstified.

The aquifer is unconfined when the limestone is in contact with unconsolidated sediments or when the water level is below the karstified zones or confined when overlapped by metapelitic rocks or clay sediments. Wells with high pumping rates concentrated in the central urban area are contributing to the formation of a large cone of depression, as shown in Figs. 7 and 6 in cross-sections 3 and 4 between wells PT-13, PT-51 and PT-46. From 1991 to 2017

Table 3. Data on the spatial distribution of each layer in the geological model.

Layer	Basement	Sete Lagoas Fm	Serra de Santa Helena Fm	Unconsolidated sediments	Karstified zone[1]	Karstified zone[2]
Area (km^2)	252	195	152	41	127	86
Elevation (m)						
Maximum	936	996	1065	1068	959	816
Minimum	467	587	627	695	538	513
Average	674	751	798	771	718	655
Standard deviation	117	72	78	44	73	60
Thickness (m)						
Maximum	-	284	218	105	129	62
Minimum	-	0	0	0	0	0
Average	-	123	51	24	14	11
Standard deviation	-	61	35	14	9	7

1. Shallow karstified zone; 2. Deep karstified zone.

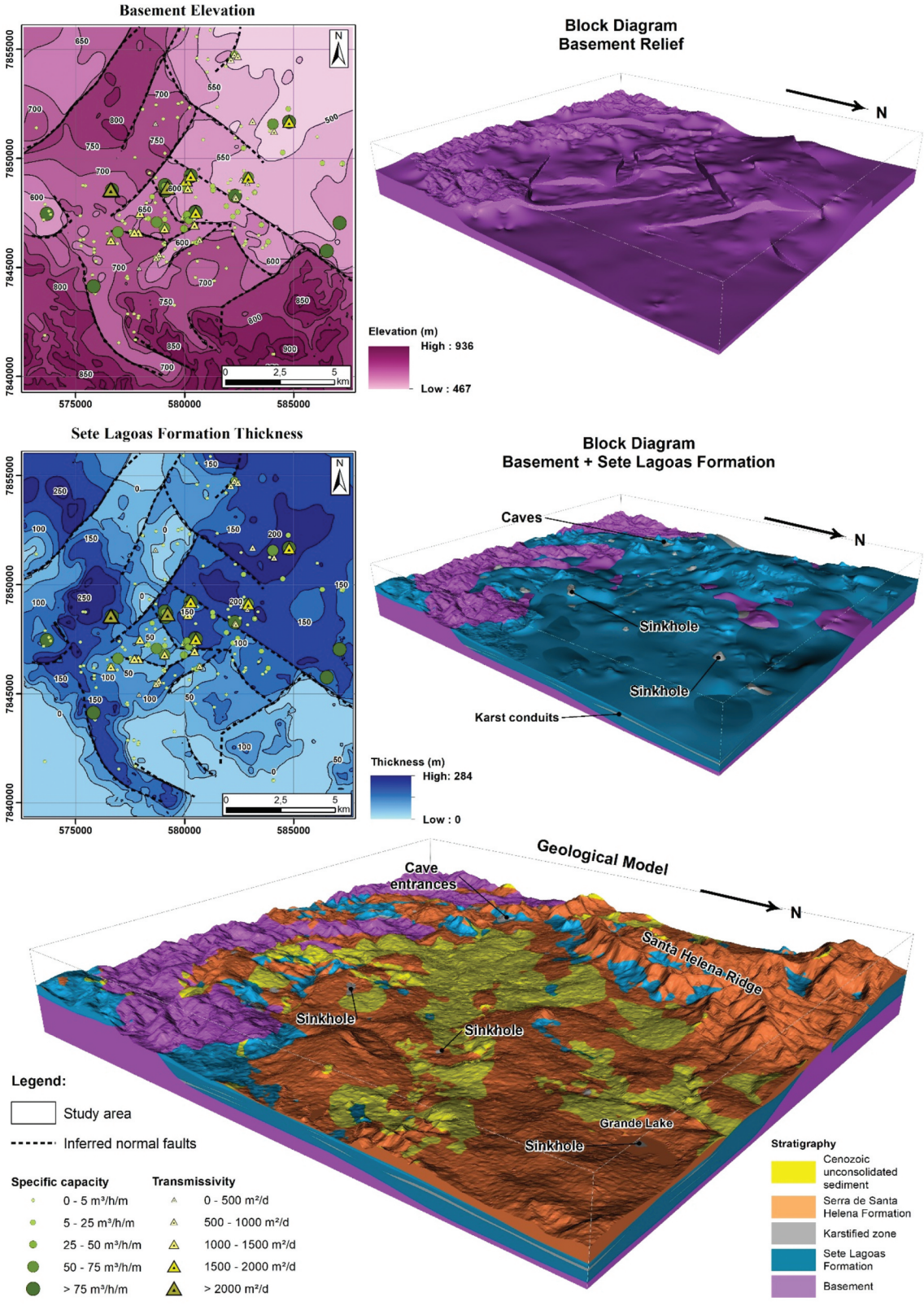

Figure 5. Diagram blocks of the geological model with the basement elevation and the Sete Lagoas Formation thicknesses.

the water level lowered up to 50 m in the most critical region, near the Paulino and José Félix lakes. This high pumping altered local natural groundwater flow directions, turning it into an artificial aquifer discharge zone, as well as changing local pressure conditions from confined to unconfined aquifer, even where there are mudstones coverage. The lowering water level makes the conduits partially saturated or even dry, concluding that the water level is below karstified zones, which was confirmed by camera inspections near Paulino lake (Galvão *et al.* 2015). This

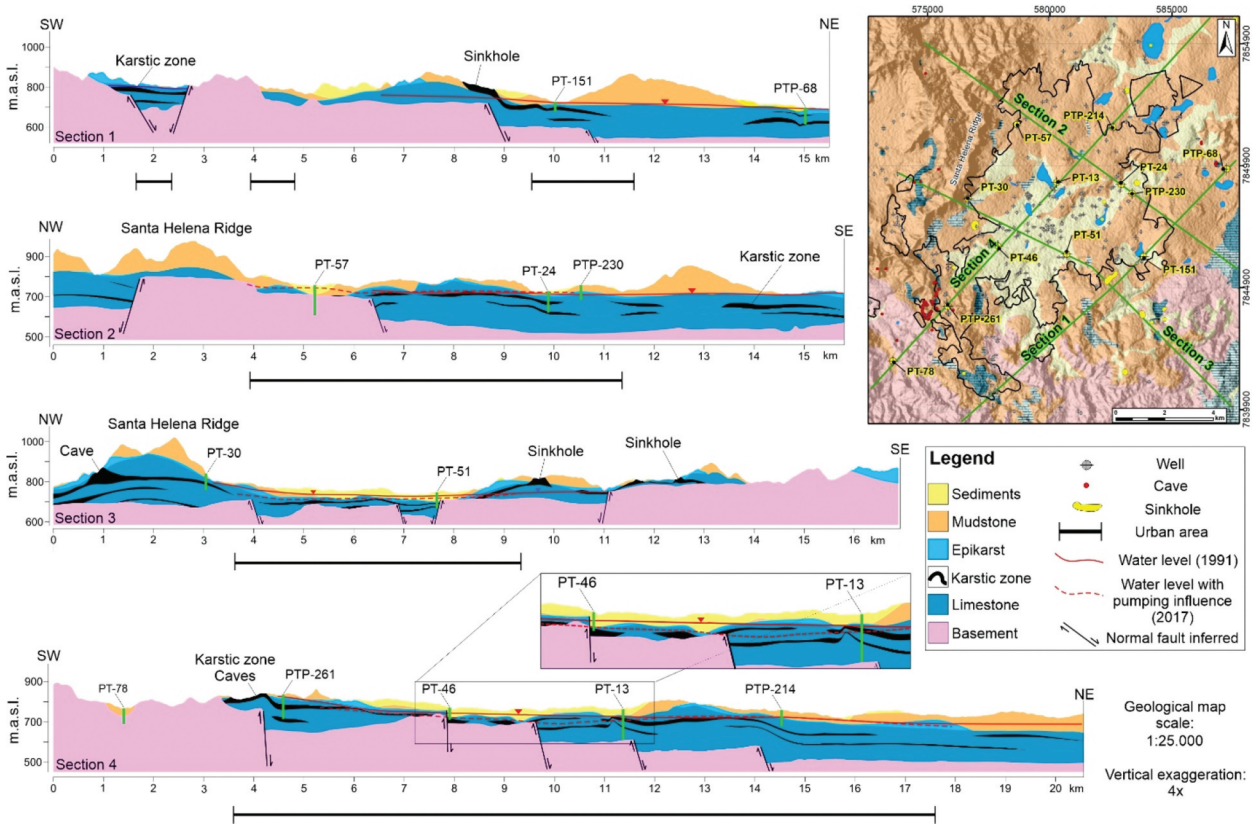

Figure 6. Hydrogeological cross-sections and representative wells with water level surfaces.

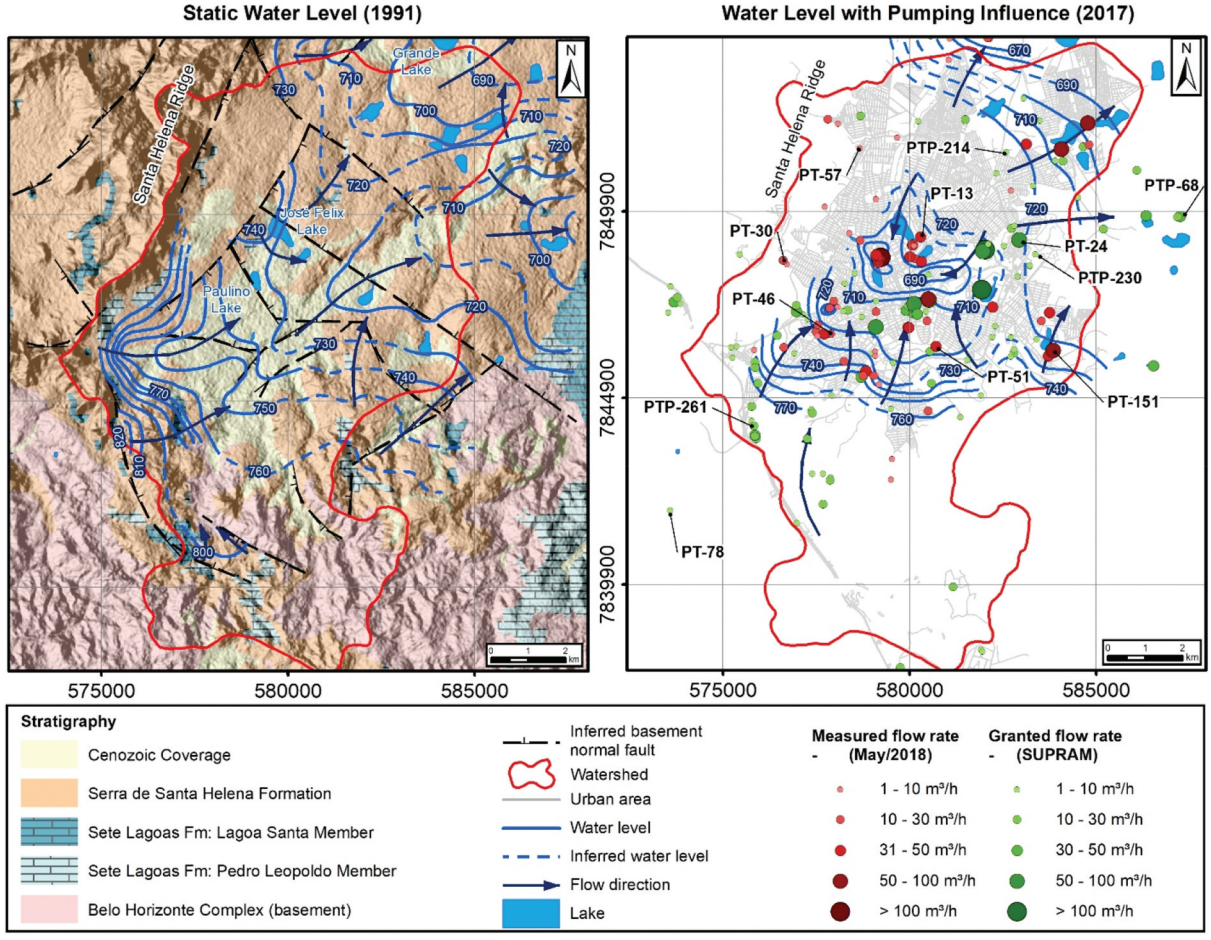

Figure 7. Potentiometric surface maps constructed via static water levels measured in tubular wells by Pessoa (1996) (left) and based on stabilized dynamic water levels measured in September 2017 (right) with the well's flow rate measured in fieldwork (red) and the flow rate granted by the Regional Environmental Superintendence (green) on license processes of public registering.

can cause great water level oscillation in karstified zone and provide sediment migration into the cavities, accelerating anthropologically the processes of subsidence and soil collapse.

However, outside the large cone of depression in the central area, there has been no significant change in water level over the years, except close to the vicinity of active pumping wells when they are in operation. The expansion of the cone of depression and the shape of its equipotential lines tend to follow the karstified zones due to the karst heterogeneity and anisotropy (Fig. 7). The alignment of lakes with local flow directions indicates they represent aquifer karst features indeed as they might be enlarged sinkholes that were filled with water and sediments.

4.4 Aquifer recharge and water balance

The recharge rates on the map in Fig. 8 are expressed as percentage of precipitation and result from the application of the APLIS method. As this method depends on the combination of 6 parameters presented in section 3.4.1, the recharge rate varies according to the weights of these parameters, resulting in 5 ranges from "very low" to "very high" recharge rate. The regions with karst features such as sinkholes, caves and fractured limestone, with higher lineament density and/or high degree of karstification, have the highest recharge rates and are usually autogenic. They can vary between 55% and 75% of precipitation, occurring during rainy season when the inflow of water is direct through limestone, without going through other lithologies or soils. The recharge rate where low karstified limestone outcrops and with lower lineament density is between 35% and 55%.

Allogenic or mixed diffuse recharge, when water percolates in regions outside the karst aquifer, such as the water derived from the basement fractured aquifer, vertical drainage via unconsolidated sediments or through mudstone open fractures, occurs, preferably, slowly during months of water surplus, from December to March. Areas with unconsolidated sediments, high lineament density and low slope have recharge rates between 35% and 55% of the precipitation, while those areas with lower lineament density and higher slopes, the recharge rate is ranging from 25% to 35%.

Due to intense fracturing of the basement rocks and their coarse-grained weathering mantle, there is a contribution of rainwater via intergranular percolation and continuous recharge in narrow valleys (Pessoa 1996), ranging from 25% to 35% of precipitation, reaching up to 40% in regions with higher lineament density. The Serra de Santa Helena aquitard can have significant water-storage capacity, but very low permeability, contributing in 1% to 5% of recharge to the karst aquifer.

Although urban areas generally affect recharge zones due to soil sealing, the municipality of Sete Lagoas is not yet very influenced by it, due to a large number of green areas and

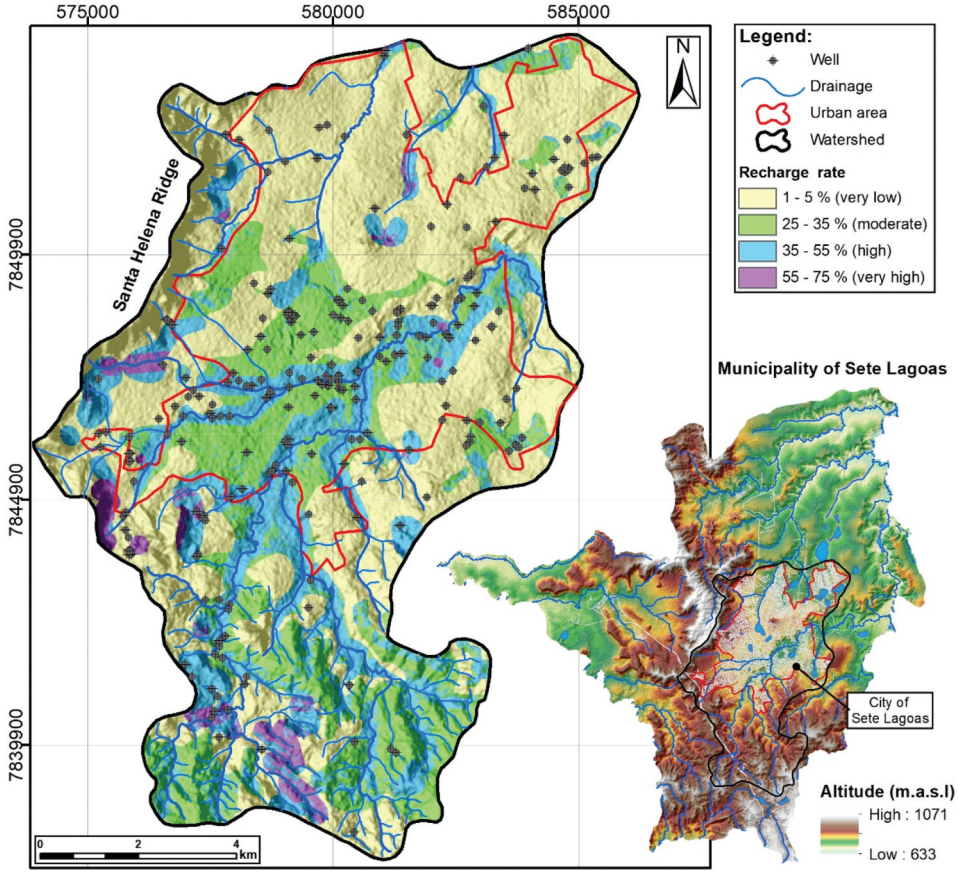

Figure 8. Recharge map used to calculate the water balance of Sete Lagoas.

exposed soil, in addition to the possible occurrence of leaks in water supply pipe system that is common in Brazilian cities (Hirata *et al.* 2019). Streams and lakes can contribute to karst aquifer recharge when the water passes through sinkholes located within them, confirmed by isotope studies and hydrochemical analyses made by Galvão *et al.* (2017) and pumping tests conducted by Assunção (2019).

The basin delimited to estimate the water balance has 120 km^2, with an average rainfall of 1321 mm/year (Table 4). The karst aquifer recharge resulted in a value of 2.88×10^7 m^3/year, equal to 18.2% of the annual precipitation or 59% of the water surplus. Withdrawal of 204 active wells corresponds to a volume of 2.41×10^7 m^3/year, equivalent to 15.2% of the annual precipitation, while minimum karst springs discharges is around $5{,}87 \times 10^5$ m^3/year or 0.4% of the annual precipitation, resulting in a total discharge of 2.47×10^7 m^3/year and 15,6% of precipitation. Subtracting the water volume of recharge by the volume of discharge, the remainder (2,6% of the precipitation) probably recharges deeper regions of the karst aquifer or flows towards the Velhas river. It means that approximately 86% of the renewable water resources in this basin is being used for the city's water supply.

Pessoa (1996) estimated a regional water balance using hydrograph river analysis to obtain the base flow and runoff of the main river of the hydrographic basin, as well as the water withdrawal by wells and the climatological water balance proposed by Thornthwaite and Mather (1955) to find other components. Although he used other methods and a bigger area to estimate the regional water balance, the results are similar to those calculated in this study if comparing percentage values, since the basins areas are different and the absolute values cannot be compared. Pessoa (1996) found the exploited volume using the average well pumping rate, the number of inhabitants and the average water consumption per inhabitant. However, as the current population is 1.56 times greater than when Pessoa's study was carried out, the current consumption should be 2.56×10^7 m^3/year of water, i.e., almost the same to that calculated in this paper, 2.41×10^7 m^3/year.

In respect of the uncertainties, there are those intrinsic to the applied methods and common to any water balance, as well as in calculation of discharge using measured and average values, but there are also some probable factors that were not included on calculations that should be highlighted. Illegal wells were not considered on calculations and they can represent a great percentage of the total as estimated by Hirata *et al.* (2019). The discharge of karst springs increases on rainy periods. The base flow calculated by Pessoa (1996), applied on both components recharge and discharge, on the main river of the hydrographic basin, also includes the discharges of other aquifers such as from unconsolidated sediments. These factors would lead to an increase of total discharge and decrease of recharge, probably resulting in a water deficit, leaving the city in an overexploitation scenario, and would explain the continuous increase of the cone of depression in the centre of Sete Lagoas since the 1990s.

4.5 Well productivity

The well productivity is represented by their specific capacity and/or transmissivity values plotted on thematic maps (Figs. 4, 5 and 9). The most productive wells (higher Q/s and/or T) are near the lakes, which are karst features that indicate groundwater flow, and close to morphostructural lineaments with E–W and NE directions within zones of higher lineament density. These lineaments correspond to open fractures that control general orientations of the main conduits.

By relating some wells (Table 5) with hydrogeological cross-sections (Fig. 6), the most productive wells are those that intercept the most karstified zones, such as wells PT-24, PTP −261, PT-13, except PT-30, which is probably related to discontinuities and connections with the Santa Helena ridge. Low-productivity wells (PT-46, PTP-214, PTP-230) are intercepting a thinner karstified zone or intercepting only the basement or mudstone rocks, such as the wells PT-78 and PT-57.

There is a concentration of more productive wells in the central region of the area, where limestones are in contact with a thick layer of Cenozoic unconsolidated sediments and limited by grabens, which makes the limestones thicker and more karstified, due to concentration of humic acid through the sediments and the basement's geometry, while less productive wells are in regions where limestones are thinner and over basement horsts (Fig. 5).

Table 4. Estimated water balance to the urban area of Sete Lagoas (left column) and the water balance estimated for the entire hydrographic basin by Pessoa (1996) (right column).

Watershed area (km^2)	Estimated water balance (2019)			Estimated water balance by Pessoa (1996)		
	120			476		
	mm/year	m^3/year	% precipitation	mm/year	m^3/year	% precipitation
Mean annual precipitation	1321	1.58×10^8	100%	1424	6.78×10^8	100%
Mean annual water surplus (a + b)	406	4.87×10^7	30.7%	478	2.28×10^8	33.6%
Mean annual evapotranspiration	915	1.10×10^8	69.3%	946	4.50×10^8	66.4%
Runoff (a)	166	1.99×10^7	12.6%	197	9.37×10^7	13.8%
Recharge (b)	240	2.88×10^7	18.2%	281	1.33×10^8	19.8%
Withdrawal by wells (c)	201	2.41×10^7	15.2%	35	1.64×10^7	2.4%
Regional base flow (d)	-	-	-	217	1.03×10^8	15.3%
Discharge of karst springs (e)	5	5.87×10^5	0.4%	-	-	-
Discharge (c + d + e)	206	2.47×10^7	15.6%	252	1.19×10^8	17.7%
Groundwater flow + storage	34	4.07×10^6	2.6%	30	1.40×10^7	2.1%

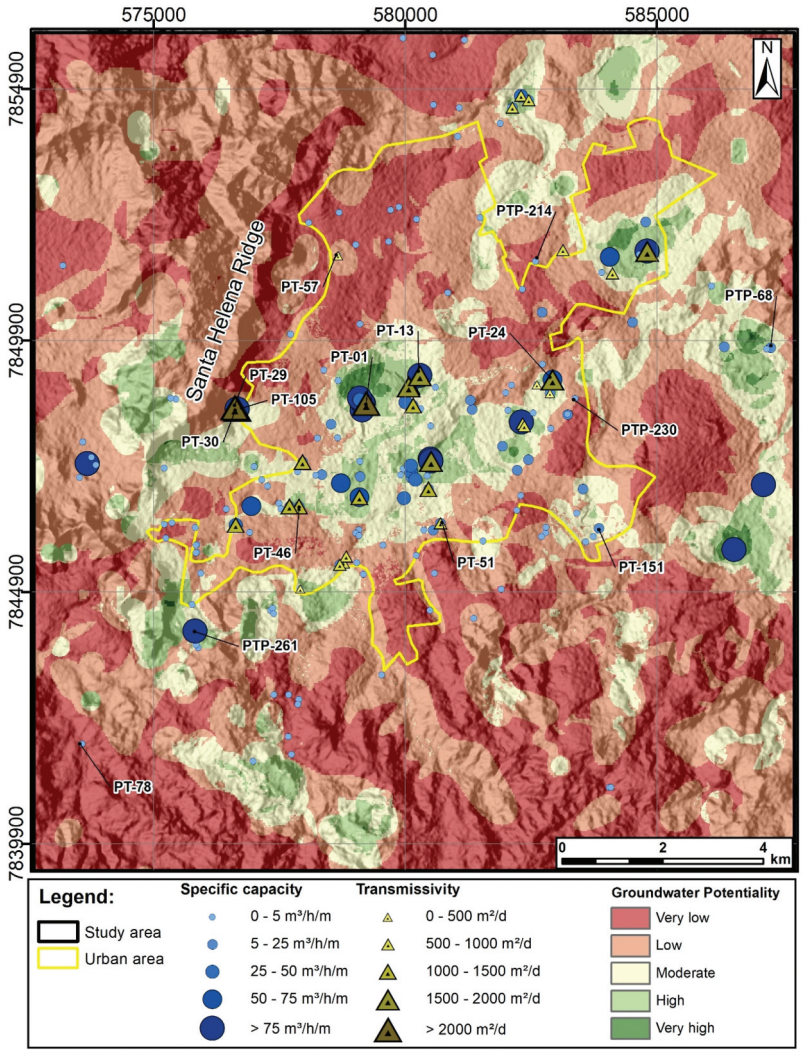

Figure 9. Groundwater potentiality map for the Sete Lagoas karst aquifer. Note that the highest values of GP coincide with the highest values of well specific capacity and aquifer transmissivities.

Table 5. Hydrodynamic features and well parameters in hydrogeological cross-sections.

Sections	Wells	Depth (m)	Specific capacity (m^3/h/m)	Transmissivity (m^2/d)	Karst zone thickness (m)
1	PT-151	132	6.8	-	15
	PTP-68	86	7.7	-	17
2	PT-57	150	0.2	450	0
	PT-24	100	73.8	1590	22
	PTP-230	75	0.3	-	0
3	PT-30	83	113.8	3590	14
	PT-51	80	5.8	930	11
4	PT-78	65	0.1	-	0
	PTP-261	120	Very high*	-	30
	PT-46	60	9.0	1020	7
	PT-13	150	128.8	1550	23
	PTP-214	80	0.1	-	0

(*) Very high specific capacity, without water level lowering during pumping test; (-) no data.

4.6 Karst groundwater potentiality

The groundwater potentiality (GP) map (Fig. 9) is a result of the analysis of four parameters: density of morphostructural and geophysical lineaments; density of surface karst features; karstified zone thicknesses in geological model; and recharge rate. These parameters are intrinsically related to structures in karst aquifer, such as faults, fractures, bedding planes, conduits and surface karst features, which are the main environments for groundwater transmission, as they are the most permeable and porous features in this type of aquifer, and therefore essential in groundwater potentiality evaluation.

The sum of these parameters indicates that the more parameters occur in an area and the greater is the weight of these parameters, the more is the GP, i.e., the more is the probability to drill a well with good productivity. As Equation (2)

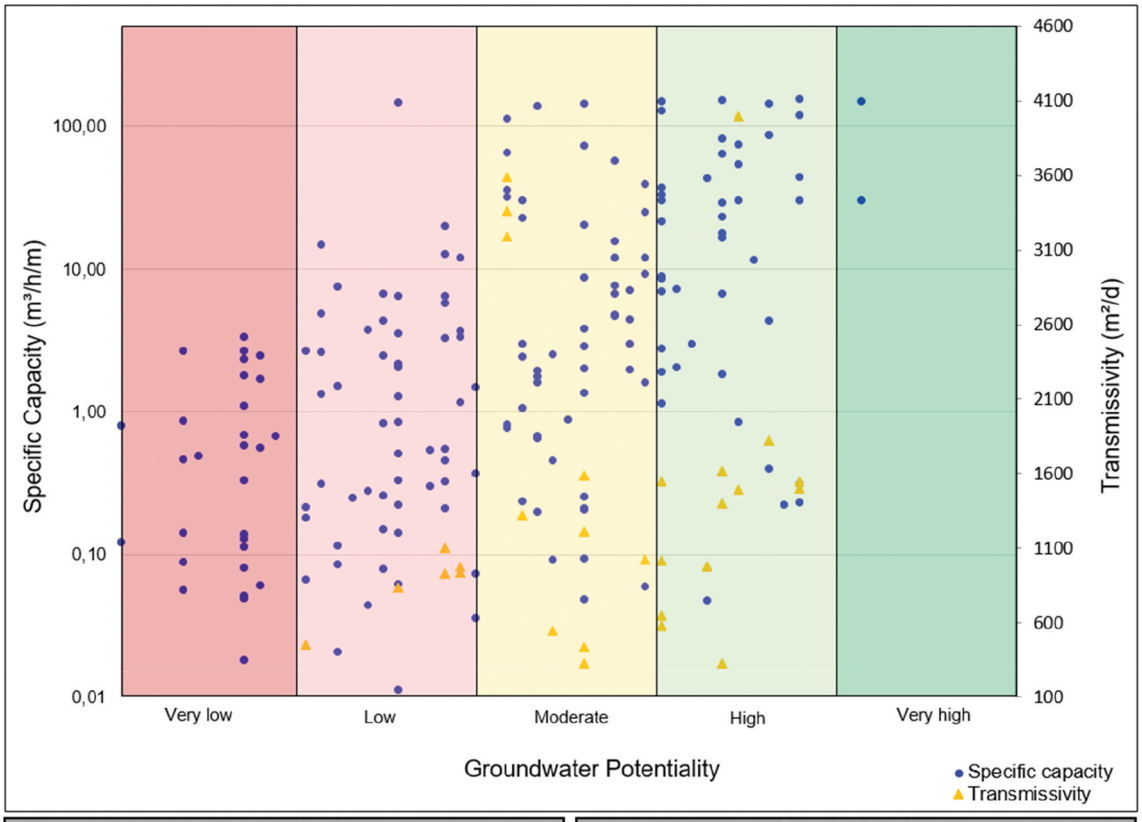

Specific capacity (m³/h/m)					
Q/s	0 - 5	5 - 25	25 - 50	50 - 75	> 75
Potentiality / nº wells	123	29	14	6	13
very low	24%	0%	0%	0%	0%
low	39%	31%	0%	0%	8%
moderate	26%	34%	36%	50%	23%
high	11%	34%	57%	50%	62%
very high	0%	0%	7%	0%	8%

Transmissivity (m²/d)					
T	0 - 500	500 - 1000	1000 - 1500	1500 - 2000	> 2000
Potentiality / nº wells	4	11	8	5	4
very low	0%	0%	0%	0%	0%
low	25%	45%	13%	0%	0%
moderate	50%	9%	38%	20%	75%
high	25%	45%	50%	80%	25%
very high	0%	0%	0%	0%	0%

Figure 10. Scatterplot and matrix of specific capacity and transmissivity values by groundwater potentiality classes.

indicates, the GP range should vary from 0, if there are no parameters on a specific area, to 4, if the four parameters are combined at the same location and with greatest weight, though the map of Fig. 9 ranges from 0 to 2.9, as there are no locations combining four parameters with very high GP classes in Sete Lagoas. However, the objective of this method is to compare and show the most potential areas to find groundwater in karst aquifer, and not compare quantitatively different areas.

In Sete Lagoas the most potential areas correspond to the central area, where limestone is covered by sediments, with enlarged conduits, making it the most karstified zone, areas with more surface karst features, especially near the lakes and sinkholes or drainages that follows structures observed in lineaments map. It is important to note that some potential areas may be on protected areas, since they are related to recharge points, which should be considered by the water resources management.

The scatter plot and matrix (Fig. 10) shows the relationship between well productivity (specific capacity, Q/s, and transmissivity, T) and groundwater potentiality. It seems to exist two groups of transmissivity values, which the highest (PT-01, PT-29, PT-30 and PT-105–see Fig. 9) present other tendency, probably because they intercept a very large saturated conduit. The growth of GP classes with increasing Q/s and T values shows that these parameters are directly proportional, attending the objective of the method applied on the production of groundwater potentiality map.

The distribution of the lowest Q/s values across the map (123 of 185 wells ranging from 0 to 5 m^3/h/m), even in more potential zones, shows how heterogeneous and anisotropic the karst aquifer is, where a dry well could be close to a highly productive one, simply because it did not intercept a saturated enlarged conduit. Therefore, although the groundwater potentiality map indicates higher-potential regions to explore groundwater in karst aquifers on a kilometre-scale map, contributing to well drilling assertiveness, it is advisable to use other investigative methods at local-scale (tens and hundreds of meters), such as local geological-structural and karst features mapping, detailed potentiometric surface mapping and local geophysics methods.

It is important to mention that the developed method was applied on a Proterozoic recrystallized limestone karst-fractured aquifer system with low primary porosity on matrix, where groundwater flows mainly in open fractures and conduits. Therefore, it may work better on karst aquifers with

similar conditions, rather than on Mesozoic karst aquifers with high primary porosity and karstification still in the initial phase.

5 Conclusions

The basement geometry in grabens and horsts with N60W, N40E and E-W mains directions, coupled with N-S compressive deformation processes on overlying formations, were the main responsible factors that controlled the geometry of hydrostratigraphic units, the karstification horizons and their directions.

The regional groundwater flow direction is to NE, with some local variations, but the concentration of wells with high pumping rates are altering the local natural groundwater flow directions, and may be causing overexploitation in the central urban area, changing some regions from confined aquifer to artificially unconfined conditions, as well as intensifying geotechnical issues such as subsidence and soil collapse.

The recharge at the basin defined for this study is around 18–20% of annual precipitation, while the discharge may reach at least 15.6%, since the illegal wells were not computed on the water balance. Therefore, the water extraction in the city of Sete Lagoas corresponds to at least 84% of the annual renewable groundwater resource, which means that the basin may be with water deficit. It is an alert for the city if no action is taken in the coming years and could significantly impact the groundwater levels in the aquifer.

Karst groundwater potentiality map proves to be an important tool for water resources management, especially for cities that depend almost entirely on groundwater, helping stakeholders to better plan urban expansions. The method to produce the map correlates four parameters, considered to be the most important in groundwater exploration on karst aquifers: morphostructural and geophysical lineaments density; density of surface karst features; thickness of karstified zone intercepted by wells; and recharge rate. It confirmed that the most productive wells are on central region of the study area, limited by grabens and over Cenozoic unconsolidated sediments, where the limestones are thicker and more karstified, on higher lineament density zones, mainly on lineaments with E-W and NE directions, intersecting thicker karstified zones and near lakes and surface karst features.

The large spatial distribution of low-productivity wells throughout the region shows how heterogeneous and anisotropic the karst aquifer is, proving the need for more detailed studies to analyse karst groundwater potentiality on local-scale, as well as the regularization of illegal wells, contributing to new data for map improvements.

Acknowledgements

Special thanks go to Coordination for the Improvement of Higher Education Personnel (CAPES) [Coordenação de Aperfeiçoamento de Pessoal de Nível Superior], to Postgraduate Program in Crustal Evolution and Natural Resources of the Department of Geology of the Federal University of Ouro Preto and to the Sete Lagoas' Water Supply and Sewage Service (SAAE) [Serviço Autônomo de Água e Esgoto]. The authors thank the *Hydrological Sciences Journal* associate editor, Professor Ghulam Jeelani, and reviewers, Dr Alan Fryar and Dr Jerome Perrin, whose comments on an earlier draft helped to improve the manuscript.

Disclosure statement

No potential conflict of interest was reported by the authors.

Funding

This work was supported by the Coordenação de Aperfeiçoamento de Pessoal de Nível Superior [R$ 1500,00].

References

Alkmim, F.F., Brito Neves, B.B., and Castro Alves, J.A., 1993. Arcabouço tectônico do Cráton do São Francisco–uma revisão (Tectonic framework of the São Francisco Craton–a review). *In*: Sociedade Brasileira de Geologia, ed. *Simpósio Cráton do São Francisco*. Salvador, Brasil: Sociedade Brasileira de Geologia, vol. 2, 45–62.

Almeida, F.F.M., 1977. O Cráton do São Francisco (The São Francisco Craton). *Revista Brasileira De Geociências*, 7 (4), 349–364. doi:10.25249/0375-7536.1977349364

Alonso-Contes, C.A., 2011. Lineament mapping for groundwater exploration using remotely sensed imagery in a karst terrain: Rio Tanama and Rio de Arecibo basins in the northern karst of Puerto Rico. Master dissertation. Michigan Technological University. http://digitalcommons.mtu.edu/etds/309.

Alves, A.S., *et al*., 2007. Sete Lagoas: a influência de uma cidade média em sua microrregião (Sete Lagoas: the influence of a medium city in its micro-region). Undergraduate thesis. PUC Minas, Contagem, Minas Gerais, Brasil.

ANA (National Water Agency), 2017. Base Hidrográfica Ottocodificada da Bacia do Rio São Francisco (Ottocodified Hydrographic Base of the São Francisco River Basin). Avaiable from: http://metadados.ana.gov.br/geonetwork/srv/pt/main.home [accessed 5 Oct 2017].

Andreo, B., *et al*., 2008. Methodology for groundwater recharge assessment in carbonate aquifers: application to pilot sites in southern Spain. *Hydrogeology Journal*, 16, 911. doi:10.1007/s10040-008-0274-5

Assunção, P.H.S., 2019. Análise da zona de recarga e sua interação com o aquífero cárstico na lagoa do matadouro, zona urbana de sete lagoas: uma abordagem científica e socioambiental (Analysis of recharge zone and its interaction with the karst aquifer in Matadouro Lake, urban area of Sete Lagoas: a scientific and socio-environmental approach). Undergraduate thesis. Federal University of Ouro Preto, Ouro Preto, MG, Brasil.

Auler, A., 1994. Hydrogeological and hydrochemical characterization of the Matozinhos-Pedro Leopoldo Karst, Brazil. Master dissertation. Western Kentucky University.

Ayer, J.E.B., Garofalo, D.F.T., and Yoshinaga, S.P., 2017. Uso de geotecnologias na avaliação da favorabilidade hidrogeológica em aquíferos fraturados (Use of geotechnologies in assessing groundwater potentiality in fractured aquifers). *Revista Águas Subterrâneas*, 31 (3), 154–167. doi:10.14295/ras.v31i3.28773

Brito, T.P., 2018. Avaliação do Potencial Hídrico de Aquíferos Fissurais dos Complexos Bação e Bonfim Setentrional, Quadrilátero Ferrífero – MG (Evaluation of Groundwater Potentiality of Fissural Aquifers from the Bação and Northern Bonfim Complexes, Quadrilátero Ferrífero–MG). Master dissertation. Federal University of Ouro Preto, MG, Brasil.

Calcagno, P., Chilès, J.P., Courrioux, G., and Guillen, A., 2008. Geological modelling from field data and geological knowledge - Part I. Modelling method coupling 3D potential-field interpolation and geological rules. *Physics of The Earth and Planetary Interiors*, 171, 147–157

CECAV (Caves National Center of Research and Conservation), 2009. National registration of speleological information. Avaiable from: https://www.icmbio.gov.br/cecav/canie.html accessesd 31 Oct 2017.

Cook, P.G., 2003. *A guide to regional groundwater flow in fractured rock aquifers*. Henley Beach, South Australia: National Library of Australia Cataloguing-in-Publication entry.

Cowan, J., *et al*. 2003. Practical implicit geological modelling. *In*: *5th International Mining Geology Conference*, November 17, 2003. Bendigo, Victoria: Australia.

CPRM, 2003. *Projeto VIDA: mapeamento geológico da região de Sete lagoas, Pedro Leopoldo, Matozinhos, Lagoa Santa, Vespasiano, Capim Branco, Prudente de Morais, Confins e Funilândia, Minas Gerais, escala 1:50.000 (Geological mapping of the Region of Sete lagoas, Pedro Leopoldo, Matozinhos, Lagoa Santa, Vespasiano, Capim Branco, Prudente de Morais, Confins e Funilândia, Minas Gerais, map scale 1:50.000)*. 2nd ed. Belo Horizonte: Brasil.

Data, C.S., 2018. Data from: Alaska satellite facility DAAC, recovered on April 27, 2018. Avaiable from: https://search.asf.alaska.edu/#/[accessed 13 Apr 2019].

Doherty, J., 2004. Model-independent parameter estimation user manual. Avaiable from: https://www.nrc.gov/docs/ML0923/ML092360221.pdf [Accessed 22 Nov 2019].

Filipponi, M., 2009. Spatial analysis of karst conduit networks and determination of parameters controlling the speleogenesis along preferential lithostratigraphic horizons. Thesis (PhD). Federal Institute of Technology of Lausanne, Switzerland.

Ford, D.C. and Williams, P.W., 2007. *Karst geomorphology and hydrology*. 2nd ed. Chichester, NY: Wiley.

Galvão, *et al*. 2016. Geologic conceptual model of the municipality of Sete Lagoas (MG, Brazil) and the surroundings. *Anais Brazilian Academy of Sciences, Rio De Janeiro*, 88 (1), 35–53. doi:10.1590/0001-3765201520140400

Galvão, P., *et al*., 2017. *Recharge sources and hydrochemical evolution of an urban karst aquifer, Sete Lagoas, MG, Brazil*. Heidelberg: Springer-Verlag Berlin. Environ Earth Sci (2017) 76:159.

Galvão, P., Halihan, T., and Hirata, R., 2015. The Karst permeability scale effect of Sete Lagoas, MG, Brazil. *Journal of Hydrology*, 531, 15–105.

Galvão, P.H.F., 2015. Modelo Hidrogeológico Conceitual de Sete Lagoas (MG) e Implicações Associadas ao Desenvolvimento Urbano em Regiões Cársticas (Conceptual hydrogeological model of Sete Lagoas (MG) and implications associated with urban development in Karst Regions). Thesis (PhD). Institute of Geosciences, University of São Paulo, São Paulo.

Goldscheider, N. and Drew, D., 2007. *Methods in Karst Hydrogeology*. Taylor & Francis, London, UK: International Contributrions to Hydrogeology.

Hassen, I., *et al*., 2016. 3D geological modelling of the Kasserine aquifer system, Central Tunisia: new insights into aquifer-geometry and interconnections for a better assessment of groundwater resources. *Journal of Hydrology*. doi:10.1016/j.jhydrol.2016.05.034

Hirata, R., *et al*., 2019. *A revolução silenciosa das águas subterrâneas no Brasil: uma análise da importância do recurso e os riscos pela falta de saneamento (The silent groundwater revolution in Brazil: an analysis of the importance of the resource and the risks due to the lack of sanitation)*. São Paulo: Instituto Trata Brasil.

Hunt, R., Doherty, J., and Walker, J., 2009. Parameter estimation and coupled groundwater/surface-water models: a PEST approach. *In*: *1st PEST Conference*, November 2009, Potomac, Maryland.

IBGE–Brazilian Institute of Geography and Statistics, 2016. Panorama de Sete Lagoas. Avaiable from: https://cidades.ibge.gov.br/xtras/perfil.php?codmun=316720 [accessed 03 Oct 2017].

INMET–National Institute of Meteorology, 2019. Meteorological and climatological station of Sete Lagoas, code OMM: 83586. Avaiable from: http://www.inmet.gov.br/portal/index.php?r=bdmep/bdmep accessed 07 Oct 2019].

Karmann, I., 1994. Evolução e dinâmica atual do sistema cárstico do alto vale do rio Ribeira de Iguape, sudeste do Estado de São Paulo (Evolution and current dynamics of the karst system in the upper valley of the Ribeira de Iguape River, southeastern of São Paulo State). Thesis (PhD). University of São Paulo, São Paulo.

Landau, E.C., *et al*., 2011. Expansão Urbana da Cidade de Sete Lagoas/MG entre 1949 e 2010 (Urban expansion of the City of Sete Lagoas/MG between 1949 and 2010). *In*: *Anais XV Brazilian Symposium on Remote Sensing–SBSR,* Curitiba, PR, Brasil, INPE, 4011–4016.

Luiz, J.G. and Silva, L.M.C., ed., 1995. *Geofísica de Prospecção (Geophysics Prospecting)*. Belém, PA, Brasil: CEJUP.

Madrucci, V., Taioli, F., and Araújo, C.C., 2008. Groundwater favorability map using GIS multicriteria data analysis on crystalline terrain, São Paulo State, Brazil. *Journal of Hydrology*, 357, 153–173. doi:10.1016/j.jhydrol.2008.03.026

Melo, M.S., and Rossetti, D.F., 2015. Morphostructural lineaments based on DEM-SRTM derivations in the Piraí Depression, State of Paraná, Southern Brazil. *Rev. Bras. Geomorf.* doi:10.20502/rbg.v16i1.615

Mendes, G.F., Sousa, R.V., and Albuquerque Filho, J.L., 2016. A relação entre a hidrogeologia e os lineamentos estruturais do planalto serrano do estado de Santa Catarina, com o uso de geotecnologias (The relationship between hydrogeology and the structural lineaments of the highlands of the state of Santa Catarina, with the use of geotechnologies). Avaiable from: https://aguassubterraneas.abas.org/asubterraneas/article/view/28677 [Accessed 7 Apr 2019].

Moura, A.C.M., *et al*., 2017. The role of vegetation cover indexes in urban areas: a contribution based on landscape ecology using sentinel-2 satellite images. *In*: *Anais of the XXVII Brazilian Congress of Cartography and XXVI Exposicarta.* Rio de Janeiro, Brazil, 1150–1155.

Niedzielski Andrea, F.A., 2013. Análise da Favorabilidade Hidrogeológica do Aquífero Multicamada Taubaté Na Região Sudoeste da Bacia Homônima (Analysis of groundwater potentiality of the Taubaté multilayer aquifer in the Southwest Region of the homonymous basin). Master dissertation, Federal University of Rio de Janeiro, COPPE/Civil Engineering Program, Rio de Janeiro.

O'Leary, D.W., Friedman, J.D., and Pohn, H.A., 1976. Lineament, linear, lineation: some proposed new standards for old terms. *U.S. Geological Survey*. doi:10.1130/0016-7606(1976)87%3C1463:LLLSPN%3E2.0.CO;2

Peñaranda, J.R., 2016. Condicionamento estrutural e litológico da porosidade cárstica da Formação Sete Lagoas, Município de Sete Lagoas (MG) (Structural and lithological conditioning of karst porosity of Sete Lagoas Formation, Municipality of Sete Lagoas (MG)). Master dissertation, University of São Paulo, SP.

Pessoa, P., 1996. Caracterização Hidrogeológica da Região de Sete Lagoas–MG: potenciais e Riscos (Hydrogeological characterization of Sete Lagoas Region–MG: potentials and risks). Master dissertation. Department of Geosciences, University of São Paulo, São Paulo.

Pessoa, P., 2005. Hidrogeologia dos aquíferos cársticos cobertos de Lagoa Santa, MG (Hydrogeology of covered karst aquifers in Lagoa Santa, MG). Thesis (PhD). Federal University of Minas Gerais, Belo Horizonte, Brasil.

Ribeiro, C.G., *et al*., 2016. Levantamento geológico estrutural aplicado aos fluxos dos aquíferos cárstico-fissurais da região da APA Carste de Lagoa Santa, Minas Gerais (Structural geological survey applied to the flows of karst-fissural aquifers in the APA Carste region of Lagoa Santa, Minas Gerais). Undergraduate thesis, Federal University of Minas Gerais, Belo Horizonte, Brasil.

Saied., P., 2008. *Development of groundwater exploration in Karst Areas using remote sensing and GIS. Map Asia 2008*. Kuala Lumpur, Malaysia: University of Waterloo, Canada. Avaiable from: https://www.researchgate.net/publication/320696500 [Accessed Jun 2019].

Salles, L., *et al*., 2018. *Evaluation of susceptibility for terrain collapse and subsidence in karst areas, municipality of Iraquara*. Chapada Diamantina (BA), Brazil: Environmental Earth Sciences. Avaiable from: https://link.springer.com/article/10.1007/s12665-018-7769-8

Thornthwaite, C.W. and Mather, J.R., 1955. *The water balance*. New Jersey: Publications in Climatology, Drexel Institute of Technology.

Tuller, M.P., *et al*., 2010. *Sete Lagoas Project–Abaeté, Minas Gerais State, Brasil. 6 geological maps, scale 1:100.000*. Belo Horizonte, Brasil: Programa Geologia do Brasil.